The role of deep soil moisture in modulating climate in the Amazon rainforest

Anna B. Harper[1], A. Scott Denning[1], Ian T. Baker[1], Mark D. Branson[1], Lara Prihodko[2], David A. Randall[1]

[1] Department of Atmospheric Science, Colorado State University, Fort Collins, Colorado

[2] Natural Resource Ecology Laboratory, Colorado State University, Fort Collins, Colorado

Abstract

Both local and large-scale processes affect the Amazon hydrologic cycle. We investigate the impact of deep soils on the atmosphere through local feedbacks. The Simple Biosphere model, version 3 (SiB3), is coupled to a single column model. Historically, land surface schemes parameterize soil moisture stress based on shallow soils and incorrectly capture seasonal cycles in the Amazon. Following observations, SiB3 is updated to allow deep roots to access soil moisture at depth. The new ("Unstressed") version of SiB3 has a stronger hydrologic cycle, with increased evapotranspiration and moisture export during the dry season. The boundary layer responds through changes in its depth, relative humidity, and turbulent kinetic energy, and these changes feed back to influence wet season onset and intensity. Differences in atmospheric latent heating could affect circulation in a global model. The results have important consequences for modeling the Amazon hydrologic cycle and climate in global climate models.

1. Introduction

Approximately half of the Amazon's evergreen forests experience dry seasons lasting at least three months [*Nepstad et al.*, 1994], and yet the forest seems to thrive during the dry, sunny months. Understanding the mechanisms that enable the forest to live through extended dry periods is of particular importance considering that changes in both climate and land use are predicted to cause a drier Amazonian climate [*Oliveira et al., 2005*].

The roots in the Amazon are well suited for dry season survival. Tap roots extend up to 11 meters deep [*Nepstad et al.*, 1994; *Jipp et al., 1998*]. Hydraulic redistribution (HR) allows the plants to access water from shallower soil layers, where most of a tree's fine roots reside, and has been observed in three trees in Brazil [*Oliveira et al.*, 2005]. These adaptations increase a plant's drought tolerance, enable the plants to maintain evapotranspiration (ET) and carbon sequestration during seasonal droughts [*Saleska et al.* 2003; *Oliveira et al., 2005*], and improve the seasonal cycles of ET and carbon fluxes in land models [*Lee et al., 2005; Baker et al.*, 2008, respectively]. However, few studies have looked at the effects of deep soils on climate in a coupled sense [e.g. *Lee et al., 2005; Kleidon and Heimann*, 1999; *Lawrence and Chase*, 2009].

Adding more realistic root and soil functions in the Simple Biosphere model, version three (SiB3), resulted in more realistic surface fluxes at certain sites in the Amazon [*Baker et al.*, 2008]. This paper aims to examine the effects of these changes on the simulated hydrologic cycle when SiB3 is coupled to a single column version of a GCM. Ultimately, SiB3 will be coupled to a global GCM. This study contributes to our understanding of the interactions between surface properties and climate in Amazonia.

Ecosystem models often incorrectly simulate fluxes of heat and moisture in the Amazon [*Saleska et al.,* 2003; *Randall et al*., 1996; *Liu,* 2004]. In coupled runs of SiB2 and CSU's GCM

(BUGS5), strong soil moisture stress led to increased Bowen ratio during the dry season [*Liu,* *2004*]. The overly strong sensible heat flux resulted in a hot, dry, and deep PBL, which diluted the incoming moisture during the subsequent wet season. Convection was inhibited and rainfall sharply decreased over the three-year simulation. The hydrologic cycle shutdown and associated ecosystem stress is analogous to the Amazon dieback found by *Cox et al.* [2004], where the forest transitioned to savannah due to decreased rainfall over western Amazonia in the 21st century [*Cox et al.*, 2004]. Similar results, albeit less dramatic, were found by *Friedlingstein et al.* [2001]. Given the potentially extreme consequences of ecosystem stress, we investigate the climatic effects of including deep roots and more realistic ecosystem stress responses in SiB3.

2. Methods

2.1 SiB

SiB is based on a land-surface parameterization scheme that computes biophysical exchanges [*Sellers et al.*, 1986] and ecosystem metabolism [*Sellers et al.,* 1996; *Denning et al.,* 1996]. SiB calculates fluxes of heat, moisture, momentum, and $CO_2$ from the gradients of each between the canopy air space (CAS) and the free atmosphere, scaled by a resistance. The monthly maximum value of the normalized difference vegetation index, from the Advanced Very High-Resolution Radiometer data, is used to derive parameters such as leaf area index and photosynthetically available radiation. The potential photosynthetic rate is scaled by these parameters, along with three stress factors that act to maximize carbon assimilation while minimizing water loss. Stress can originate from less than optimal temperature, canopy air space humidity, and soil moisture. This study focuses on the latter.

We compare two versions of SiB3, S3_Stressed and S3_Unstressed, which have four main differences. The latter version corresponds to the deep soil SiB3 discussed in *Baker et al.* [2008].

The root depths are 3.5 and 10 meters in S3_Stressed and S3_Unstressed, respectively, allowing the latter to hold more soil moisture. In S3_Stressed transpired water is removed from the soil based on root fractions in each layer, which does not account for the importance of hydraulic redistribution and deep roots. Although root density is low in the deepest layers, most of the water resides in these layers. The ability of deep roots to access large amounts of water has been observed [*Jipp et al.,* 1998, *Nepstad et al.*, 1994, e.g.]. In S3_Unstressed, transpired water is removed from an "apparent" root fraction, accounting for both actual root fraction and moisture content in each layer.

In S3_Stressed, soil moisture stress increases rapidly once soil moisture drops below the wilting point. This response is realistic on a plant-by-plant basis. However, in reality soil moisture and water table depth can vary greatly within a grid cell, and not all plants reach the wilting point at the same time. Therefore, in S3_Unstressed, soil moisture stress increases more gradually in response to decreasing soil moisture. Finally, the optimum soil moisture for heterotrophic respiration is increased from 67% to 75% of saturation in S3_Unstressed, which is more in line with observations in the Amazon [*Baker et al.,* 2008].

2.2 SCM

We performed numerical simulations using a single-column version (SCM) of BUGS5, an atmospheric GCM that has evolved from the 1980's UCLA GCM. The model uses a modified sigma coordinate with a prognostic planetary boundary layer (PBL) [*Randall et al.,* 1985]. The PBL depth changes due to horizontal mass flux divergence, entrainment of air from above the PBL, and loss of mass due to convection. The entrainment rate is predicted by integrating the turbulent kinetic energy (TKE) conservation equation over the depth of the PBL [*Denning et al.*, 2008]. Positive entrainment occurs due to production of TKE by buoyancy and shear, while

consumption by downward buoyancy fluxes and dissipation of TKE reduce entrainment. The PBL depth is constrained to be between 10 and 160 hPa.

BUGS5 uses a modified Arakawa-Schubert cumulus parameterization with prognostic closure [*Ding and Randall*, 1998], and cloud microphysics as described by *Fowler and Randall* [2002]. The radiative transfer scheme is based on *Gabriel et al.* [2001] and *Stephens et al.* [2001]. Aerosol loading is assumed to be light during the wet season, and heavier during the late dry season when fires are common. Values for aerosol optical thickness, single scattering albedo, and asymmetry factor are assigned as in Table 1 based on observations from *Franchito et al.* [2002], *Andreae et al.* [2002], *Schafer et al*. [2002], and *Tarasova et al.* [1999].

Horizontal advective tendencies of temperature and water vapor are prescribed using relaxation forcing [*Randall and Cripe,* 1999]. Profiles of temperature and water vapor are relaxed toward their observed upstream values, scaled by a relaxation timescale. Relaxation forcing guarantees that the modeled soundings of the state variables will be realistic and enables comparisons of SiB's results to surface observations of fluxes of heat, moisture, and carbon dioxide.

The SCM is forced by six-hourly NCEP Reanalysis II [*Kalnay and Kanamitsu*, 1996]. Since the footprint of the column (2.5° x 2.5°) is larger than the footprint of the tower, we do not expect the model to exactly mimic the observations at the KM83 tower, but we do expect the same seasonal cycles. We run the model from 2001-2003 five times to allow for soil moisture spin-up. The results shown are from the fifth iteration.

2.3 Site Description

The flux tower in the Tapajos National Forest was operated from 2001 to 2004 as part of the Large-scale Biosphere-Atmosphere Experiment in Amazonia (LBA), an international

research initiative led by Brazil. The tower is near the kilometer 83 marker on the Santarem-Cuiaba highway (BR 163), approximately 70 km south of Santarem, in Para, Brazil (3.01°S, 54.58°W). Data from the tower includes half-hourly measurements of air temperature, precipitation, radiation, and fluxes of heat and water vapor. The experimental design and instrumentation are fully described by *Goulden et al.* [2004], *da Rocha* [2004], and *Miller et al.* [2004].

3. Results

3.1 Seasonal hydrologic cycle

In S3_Stressed, evaporation has a strong seasonal cycle due to increased ecosystem stress in the dry season. Evaporation is sustained through the dry season in S3_Unstressed because of the plants' ability to access deep soil moisture throughout the entire rooting profile. In this version of the model, the forest transports moisture away from areas of sustained ET. The dry season precipitable water content is 0.6 to 1.6 mm higher, and moisture advection is 1-2 mm day$^{-1}$ stronger compared to S3_Stressed (Fig. 1b,d). The monthly rainfall totals are not strongly affected by these changes, and modeled and observed rainfall is similar in both versions of the model (Fig. 1a).

The stronger hydrologic cycle in S3_Unstressed is consistent with observations. The plot of P-E (Fig. 1e) represents our best estimate of the observed hydrologic cycle at the tower. Calculated advection from NCEP Reanalysis variables is also shown in Figure 1d. S3_Unstressed is within the range of the observations during most months, and particularly during the dry seasons.

3.2 Seasonal heat and moisture fluxes

Simulated fluxes of sensible and latent heat are compared to tower observations in Figure

2. The seasonal cycles of latent and sensible heat are too strong in S3_Stressed. The errors are largest during the dry season, when latent heat is too low and sensible heat is too high. The seasonal cycle of latent heat flux is more realistic in S3_Unstressed, consistent with results from *Baker et al.* [2008], who showed that similar changes in an offline version of SiB3 resulted in improved fluxes of $CO_2$ at the same site.

The differences between S3_Stressed and Unstressed have important implications for simulating the regional climate. The canopy air space is cooler and more moist in S3_Unstressed, although these variables are overestimated compared to observations. During the dry season, weaker PBL buoyancy and shear result in less TKE production and a generally shallower PBL in S3_Unstressed (Fig. 2f). Because of the decreased PBL depth and temperature and increased PBL moisture, it is unlikely that S3_Unstressed will produce a hydrologic shutdown like that in SiB2/BUGS5 [*Liu,* 2004]. The improvements in S3_Unstressed could improve simulations of precipitation and moisture fluxes in a global coupled GCM.

3.3 Dynamical implications

Increased atmospheric moisture can result in increased condensation and latent heating. S3_Unstressed consistently has stronger atmospheric heating during the dry season from the surface to 500 hPa. During the wet season, S3_Unstressed (S3_Stressed) has stronger heating from 400-600 hPa (from 700-925 hPa and from 200-300 hPa). The differences in atmospheric heating between the models have important implications for the local and regional circulation. In the tropics, a heating source aloft is balanced primarily by upward motion, which must be compensated for by descending air elsewhere [*Hoskins and Karoly*, 1981]. It is not unreasonable to expect that using S3_Unstressed in a global model will result in stronger dry season atmospheric heating throughout the Amazon. This would result in stronger rising motion above

the basin, a low-level vorticity source and an enhanced surface trough to the west [*Hoskins and Karoly*, 1981]. The increased low-level moisture in S3_Unstressed results in higher vertically integrated moist static energy and weaker gross moist stability during most months of the simulation, consistent with the results of a stronger hydrologic cycle in this version of the model.

3.4 Wet season characteristics

Wet season onset is defined as the first pentad with greater than 3.33 mm day$^{-1}$ of rain, where four of the following six pentads are above and four of the previous six pentads are below the threshold [*Li and Fu,* 2004] (Table 2). Figure 3 shows the evolution of the PBL, rainfall, and moisture advection during the transition between dry and wet seasons. Prior to wet season onset, S3_Unstressed has lower surface sensible heat flux and buoyancy, leading to lower TKE production and entrainment at the PBL top. Both versions of the model relax to the same upstream water vapor profile, but in S3_Unstressed the PBL is less diluted by free tropospheric air, surface evaporation is higher, and hence the PBL relative humidity is higher.

In the model, the degree to which these factors influence wet season characteristics is related to the relative importance of local and large-scale processes. In 2002, the wet season begins 25 days earlier in S3_Unstressed compared to S3_Stressed (Fig. 3e). Throughout the wet season, the mean entrainment rate and PBL depth are lower, evaporation is higher, and the rainfall rate is higher (Fig. 3 does not show the full wet season). In late 2002 and early 2003, the upstream profile is drier than the previous year. During the 2003 wet season, the PBL is deeper in S3_Unstressed, and evaporation and precipitation are lower. In both dry seasons, the rainfall intensity is more realistic in S3_Unstressed, although cumulative wet season rainfall is more realistic in S3_Stressed in 2003 and both models end the wet season too early (Table 2).

4. Discussion and Conclusions

This study highlights the importance of root-zone processes in the hydrologic cycle and circulation of the Amazon region. Previous versions of SiB and other ecosystem models parameterize root-zone moisture stress based on shallow soils where roots can only access water in their respective layers. This study and others [*Baker et al.,* 2008; *Liu,* 2004] show that such parameterizations do not accurately capture the seasonal cycles of heat, moisture, and carbon dioxide fluxes at sites throughout the Amazon. The changes made to SiB3 are motivated by observations in the Amazon and differ from historical land surface treatments in the tropics. In the single column model, all large-scale dynamics are constrained by NCEP II reanalysis and therefore the model's effect on the atmosphere is limited to local processes. Despite this, the changes to the land surface affect the hydrologic cycle, boundary layer, tropospheric dynamics, and wet season characteristics. The improved surface representation will likely affect the large-scale circulation and regional hydrologic cycle if implemented into a fully coupled GCM.

Acknowledgements

References

Andreae, M.O., et al. (2002), Biogeochemical cycling of carbon, water, energy, trace gases, and aerosols in Amazonia: The LBA-EUSTACH experiments, *J. Geophys. Res., 27*(D20), doi: 10.1029/2001JD000524.

Baker, I.T., L. Prihodko, A.S. Denning, M. Goulden, S. Miller, and H.R. da Rocha (2008), Seasonal Drought Stress in the Amazon: Reconciling Models and Observations, *J. Geophys. Res.*, *113*, G00B01, doi: 10.1029/2007GJ000644.

Denning, A.S., et al. (1996), Simulations of Terrestrial Carbon Metabolism and Atmospheric $CO_2$ in a General Circulation Model. Part I: Surface Carbon Fluxes. *Tellus*, *48B*, 521-542.

Denning, A.S., et al. (2008) Evaluation of modeled atmospheric boundary layer depth at the WLEF tower. *Agricultural and Forest Meteor., 148(2)*, doi: 10.1016/j.agrformet.2007.08.012

Ding, P., and D. A. Randall (1998), A Cumulus Parameterization with Multiple Cloud Base Levels. *J. Geophys. Res.*, *103*(D10), 11,341-11,354.

Fowler, L. D., and D. A. Randall (2002), Interactions between cloud microphysics and cumulus convection in a general circulation model. *J. Atmos. Sci.*, *59*, 3074-3098.

Franchito, S.H., E.C. Moraes, and V. Brahmananda Rao (2002), Simulations with a radiation model and comparisons with LBA data sets. *J. Geophys. Res., 27*(D20), doi: 10.1029/2001JD001356.

Gabriel, P.M., P.T. Partain, and G.L. Stephens (2001), Parameterization of Atmospheric Radiative Transfer. Part II: Selection Rules. *J. Atmos. Sci.*, *58*(22), 3411-3423.

Goulden, M.L., S.D. Miller, M.C. Menton, H.R. da Rocha, and H.C. Freitas (2004), Diel and seasonal patterns of tropical forest $CO_2$ exchange. *Ecological Applications*, *14*(4), S42-

S54.

Hoskins, B.J. and D.J. Karoly (1981), The steady linear response of a spherical atmosphere to thermal and orographic forcing. *J. Atmos. Sci.*, *38*, 1179-1196.

Huete, A.R., et al. (2006), Amazon rainforests green-up with sunlight in dry season. *Geophys. Res. Lett.*, *33*, L06405, doi:10.1029/2005GL025583.

Jipp, P.H., D.C. Nepstad, D.K. Cassel, and C.R. de Carvalho (1998), Deep soil moisture storage and transpiration in forests and pastures of seasonally-dry Amazonia. *Climatic Change*, *39*, 395-412.

Kalnay, E., et al. (1996), The NCEP/NCAR 40-year Reanalysis project. *Bull. Amer. Meteor. Soc.*, *77*(3), 437-471.

Kleidon, A. and M. Heimann (1999), Deep-rooted vegetation, Amazonian deforestation, and climate: results from a modeling study. *Glob. Ecol. and Biogeog. 8*, 397-405.

Lawrence, P.J. and T.N. Chase (2009), Climate impacts of making evapotranspiration in the Community Land Model (CLM3) consistent with the Simple Biosphere model (SiB), *J. Hydrometeor.*, *10*(2), doi: 10.1175/2008JHM987.1.

Lee, J.E., R.S. Oliveira, T.E. Dawson, and I. Fung (2005), Root functioning modifies seasonal climate, *PNAS*, *102*(49), 17576-17581, doi: 10.1073/pnas.0508785102.

Li, W. and R. Fu (2004), Transition of the large-scale atmospheric and land surface conditions from the dry to the wet season over Amazonia as diagnosed by the ECMWF Reanalysis. *J. Clim.*, 2637-2651.

Liu, J. (2004), Investigation of ecosystem drought stress and its impacts on carbon exchange at tropical forests, M.S. thesis, Colo. State Univ., Fort Collins.

Miller, S.D., et al. (2004), Biometric and Micrometeorological Measurements of Tropical Forest

Carbon Balance, *Ecological Applications*, *14*(4), S114-S126.

Nepstad, D.C., et al. (1994), The role of deep roots in the hydrological and carbon cycles of Amazonian forests and pastures. *Nature*, *372*, 666-669.

Oliveira, R.S., T.E. Dawson, S.S.O. Burgess, and D.C. Nepstad (2005), Hydraulic redistribution in three Amazonian trees. *Oecologia*, *145*, 354-363, doi: 10.1007/s00442-005-0108-2.

Randall, D.A., J.A. Abeles, and T.G. Corsetti (1985), Seasonal simulations of the planetary boundary layer and boundary layer stratocumulus clouds with a general circulation model. *J. Atmos. Sci.*, *42*, 641-676.

Randall, D.A., et al. (1996), A Revised Land-Surface Parameterization (SiB2) for Atmospheric GCMs. Part 3: The Greening of the CSU General Circulation Model. *J. Clim.*, *9*, 738-763.

Randall. D.A. and D.G. Cripe (1999), Alternative Methods for Specification of Observed Forcing in Single-Column Models and Cloud System Models. *J. Geophys. Res.*, *104*(D20), 24,527-24,545.

da Rocha, H.R., et al. (2004), Seasonality of water and heat fluxes over a tropical forest in eastern Amazonia. *Ecological Applications*, *14*(4), S22-S32.

Saleska, S.R., et al. (2003), Carbon in Amazon forests: Unexpected seasonal fluxes and disturbance-induced losses. *Science*, *302*, 1554-1557, doi: 10.1126/science.1091165.

Schafer, J.S., B.N. Holben, T.F. Eck, M.A. Yamasoe, and P. Artaxo (2002), Atmospheric effects on insolation in the Brazilian Amazon: Observed modification of solar radiation by clouds and smoke and derived single scattering albedo of fire aerosols. *J. Geophys. Res.,* *107*(D20), doi: 10.1029/2001JD000428.

Sellers, P.J., Y. Mintz, Y.C. Sud, and A. Dalcher (1986), A Simple Biosphere Model (SiB) for

Use within General Circulation Models. *J. Atmos. Sci.*, *43*(6), 505-531.

Sellers, P.J., et al. (1996), A Revised Land Surface Parameterization (SiB2) for Atmospheric GCM's. Part I: Model Formulation. *J. Clim.*, *9*(4), 676-705.

Stephens, G.L, P.M. Gabriel, and P.T. Partain (2001), Parameterization of Atmospheric Radiative Transfer. Part I: Validity of Simple Models. *J. Atmos. Sci.*, *58*(22), 3391-3409.

Tarasova, T.A., C.A. Nobre, B.N. Holben, T.F. Eck, and A. Setzer (1999), Assessment of smoke aerosol impact on surface solar irradiance in the Rondonia region of Brazil during Smoke, Clouds, and Radiation – Brazil. *J. Geophys Res., 104*(D16), 19161-19170.

|  | Wet season | Transition season | Dry season |
|---|---|---|---|
| Optical thickness (SW) | 0.05 | .08 | .10 |
| Single scattering albedo (SW) | .989 | .989 | .989 |
| Asymmetry factor (SW) | .743 | .743 | .743 |
| Optical thickness (LW) | 0.03 | .04 | .1 |
| Single scattering albedo (LW) | .696 | .696 | .588 |
| Asymmetry factor (LW) | .779 | .779 | .631 |

Table 1 Aerosol optical properties. Based on preliminary model runs, the wet season is January

through June, the transition season is July and August, and the burning season is September

through December.

| | S3_Stressed | S3_Unstressed | KM83 |
|---|---|---|---|
| **2002 dates** | Jan. 25 – June 8 | Jan. 1 – June 18 | Jan. 10 – June 28 |
| **2002 rainrate (mm day$^{-1}$)** | 5.87 | 6.04 | 6.25 |
| **2002 total rainfall (mm)** | 821 | 966 | 1062 |
| **2003 dates** | Jan. 15 – May 5 | Jan. 20 – May 5 | Jan. 25 – June 13 |
| **2003 rainrate (mm day$^{-1}$)** | 8.22 | 7.70 | 6.47 |
| **2003 total rainfall** | 945 | 847 | 938 |

Table 2: Comparison of wet season characteristics between S3_Stressed, Unstressed, and

observations at KM83.

Figure 1. Monthly mean composites of the hydrologic cycle. In D), comparison is made to moisture advection calculated from NCEP Reanalysis precipitation, evaporation, and precipitable water.

Figure 2. Comparison of modeled and (when available) observed variables. In G and H, NCEP II Reanalysis values are from 1000 hPa and the tower observations are from a height of 10 meters.

Figure 3. Pentad-averaged values for NDJFM of PBL depth (A,B), entrainment at the PBL top (C,D), precipitation rate (E,F), vertically averaged moisture advection (G,H), and PBL relative humidity (I,J). The solid (dashed) vertical lines indicate pentad of wet season onset in S3_Unstressed (S3_Stressed). In G and H, the dotted line indicates the threshold rain rate for wet season onset (3.33 mm/day).
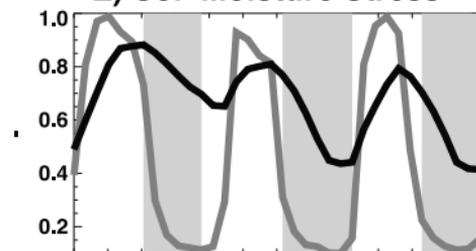
**A) Precipitation**
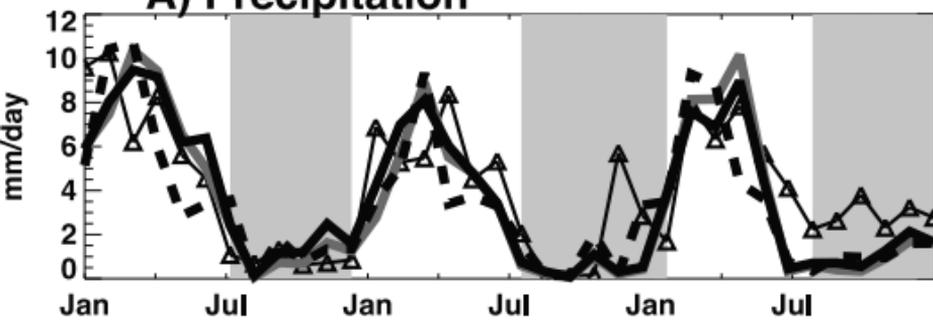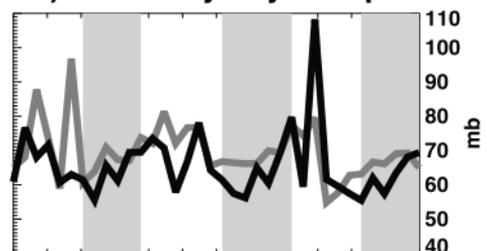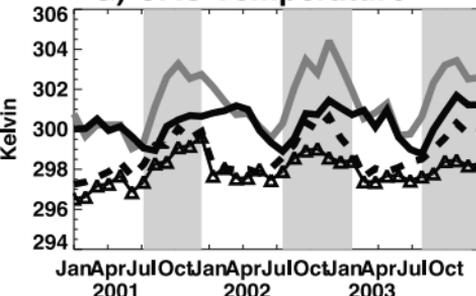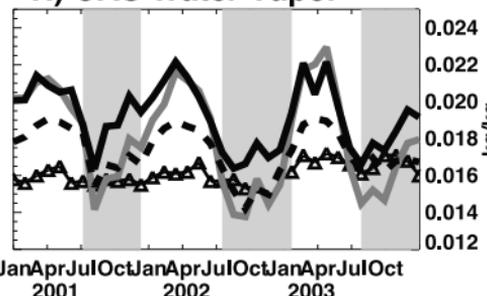
**B) Precipitable Water**
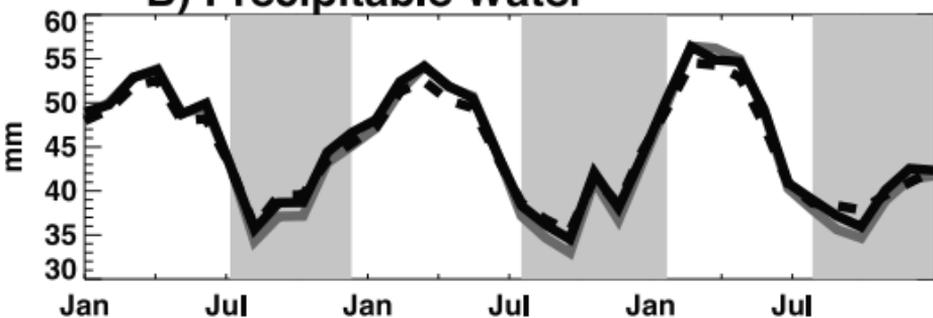
**C) Evaporation**
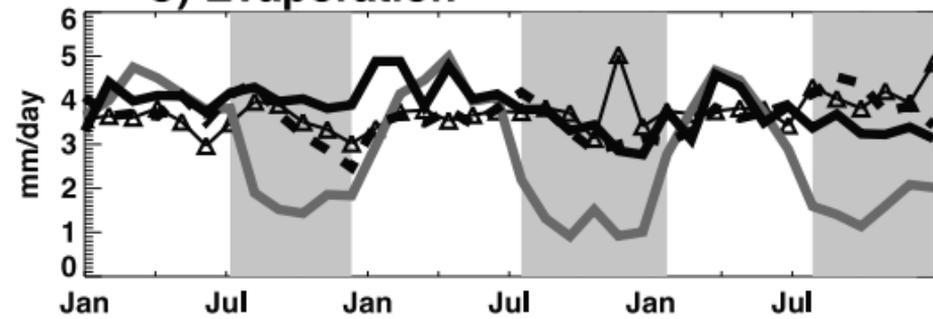
**D) Moisture Advection**
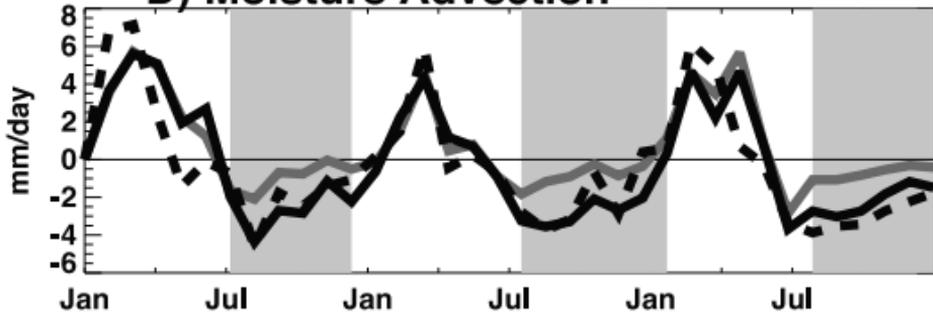
**E) Precipitation-Evaporation**
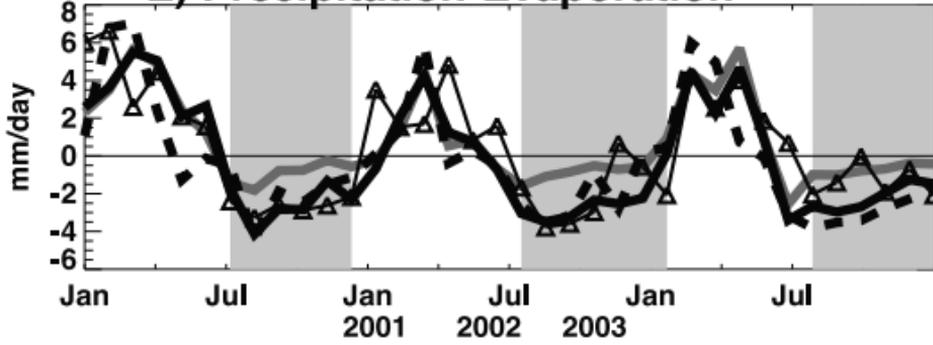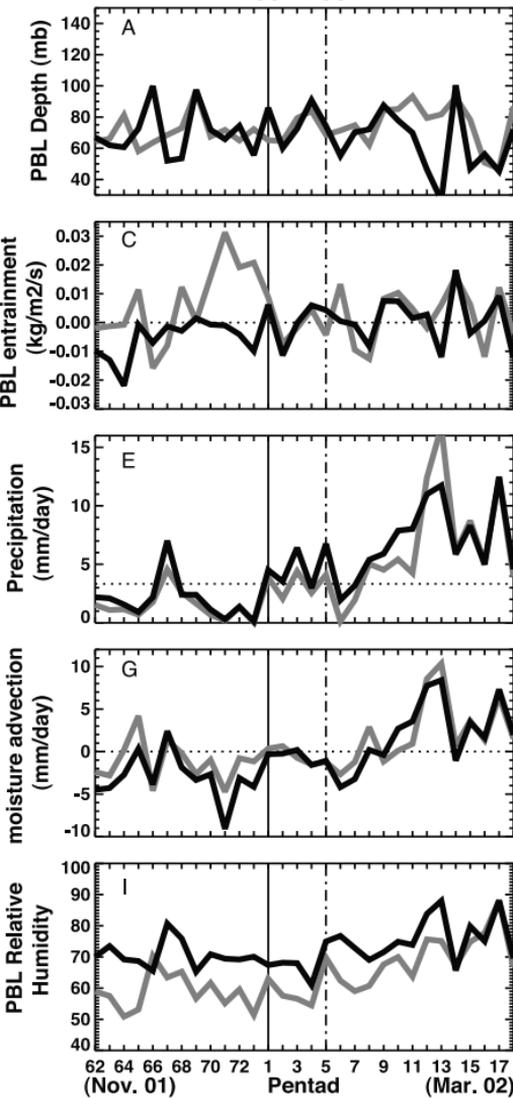
SiB3 Stressed   SiB3 Unstressed   KM83 Observations   NCEP II Reanalysis

A) Sensible Heat
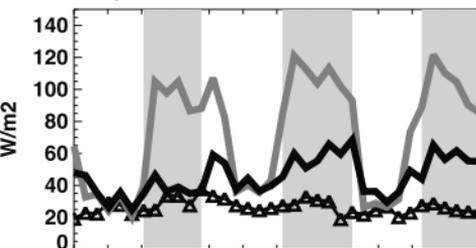
B) Latent Heat
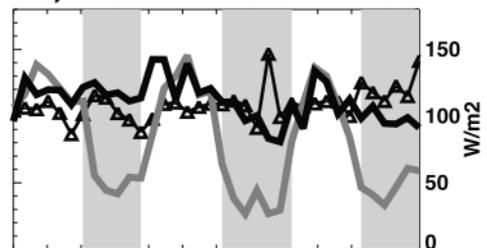
C) Bowen Ratio
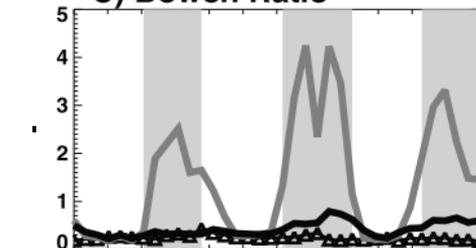
D) Net Radiation @ Surface
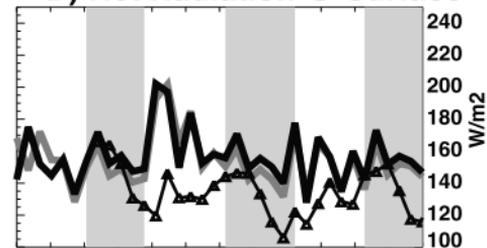
E) Soil Moisture Stress

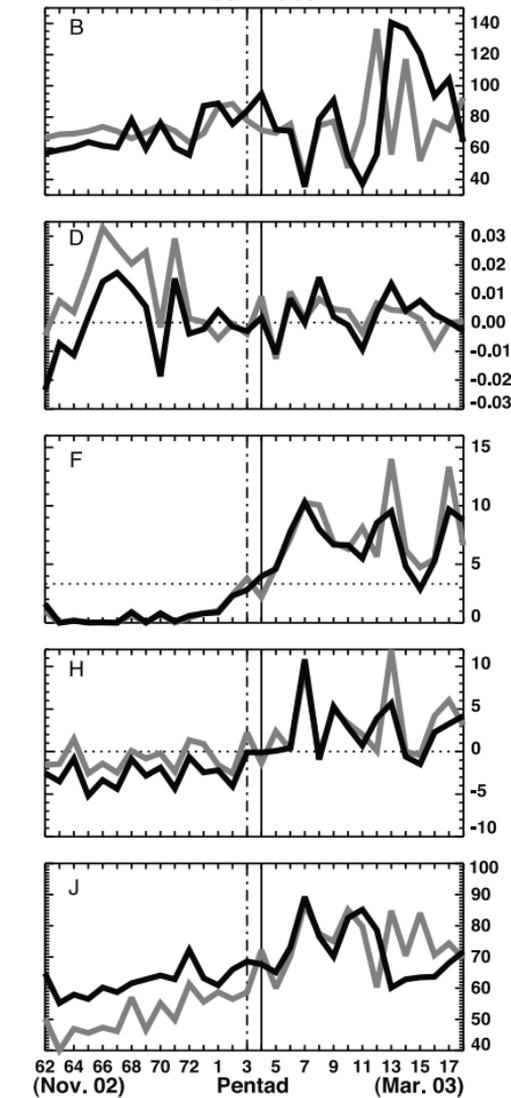F) Boundary Layer Depth

G) CAS Temperature

H) CAS Water Vapor

SiB3 Stressed          SiB3 Unstressed          KM83 Observations          NCEP II Reanalysis

2001-2002                    2002-2003

A — PBL Depth (mb)          B

C — PBL entrainment (kg/m2/s)   D

E — Precipitation (mm/day)   F

G — moisture advection (mm/day)   H

I — PBL Relative Humidity   J

62 64 66 68 70 72  1 3 5 7 9 11 13 15 17
(Nov. 01)      Pentad      (Mar. 02)

62 64 66 68 70 72  3 5 7 9 11 13 15 17
(Nov. 02)      Pentad      (Mar. 03)

S3_Stressed          S3_Unstressed